Controlling the Morphology of Amorphous Solid Water

K. P. Stevenson,* Greg A. Kimmel,* Z. Dohnálek,* R. Scott Smith, Bruce D. Kay†

The morphology of amorphous solid water grown by vapor deposition was found to depend strongly on the angular distribution of the water molecules incident from the gas phase. Systematic variation of the incident angle during deposition using a collimated beam of water led to the growth of nonporous to highly porous amorphous solid water. The physical and chemical properties of amorphous solid water are of interest because of its presence in astrophysical environments. The ability to control its properties in the laboratory may shed light on some of the outstanding conflicts related to this important material.

Amorphous solid water (ASW) is the most abundant phase of water in astrophysical environments, where it is believed to be a major component of comets (*1*), planetary rings (*2*), and interstellar clouds (*3*). ASW is also a metastable extension of liquid water (*4*) and as such is a model system for studying deeply supercooled liquids (*5*). Consequently, the physical and chemical properties of ASW, which are intimately related to its morphology, are of considerable interest to physical chemists, astrophysicists, planetary scientists, and cryobiologists. The growth and annealing temperatures are well known to strongly influence the physical properties of ASW. Nevertheless, conflicting results, which have been reported for such fundamental properties as the surface area (*6–11*), density (*1, 12–17*), and porosity (*7, 16, 17*) of ASW, remain unresolved. Here, we show that the angular distribution of the incident water molecules is as important as the temperature in determining the morphology of ASW.

We have investigated the morphology of thin ASW films deposited by two different methods: from highly collimated, effusive H_2O beams and from ambient vapor. Deposition rates of 0.02 to 0.12 bilayer per second were used in both cases (1 bilayer $\approx 1.1 \times 10^{15}$ molecules per square centimeter). The angular divergence of the collimated beams was ~0.2° (half angle). The films were deposited on a Pt(111) crystal in the temperature range 22 to 145 K. The beam-deposited ASW films have a region of uniform thickness (the umbra) surrounded by a region of decreasing thickness (the penumbra), whereas films grown from ambient vapor are uniform across the entire sample. The uniformity of the films was verified by Auger electron spectroscopy and temperature-programmed desorption (TPD) of the ASW.

The ASW films were characterized by their saturation coverage of N_2 at 26 K, which was measured by integrating the TPD line shapes obtained with a quadrupole mass spectrometer. The information obtained is analogous to that from N_2 Brunauer-Emmett-Teller (BET) isotherm measurements (*18*) but allows ASW films to be studied at temperatures much lower than 77 K. The N_2 gas was deposited normal to the surface using a supersonic beam that was smaller than, and centered on, the umbra of the ASW film. N_2 uptake was independent of incident angle. At 26 K, the N_2 will adsorb on the surface of the ASW and in pores, but it will not form multilayers on a flat surface. We have experimentally verified that N_2 diffusion on the surface and through the pores of the ASW deposit is very rapid, ensuring uniform coverage of the film. The curvature of the pores locally reduces the N_2 vapor pressure, allowing multilayer adsorption (capillary condensation) in pores below some maximum radius (*18*). Therefore, the amount of N_2 adsorption is a measure of the accessible surface area and pore volume of the film. Water deposited at temperatures above 140 K resulted in nonporous crystalline ice. The area of the monolayer N_2 TPD signal from crystalline ice was used as a reference state for normalizing the N_2 adsorption in ASW.

The amount of N_2 adsorbed by 50-bilayer ASW films grown at 22 K on Pt(111) versus the deposition angle, θ, is shown in Fig. 1. N_2 adsorption by ASW films grown with $\theta \leq 20°$ was similar to adsorption by a crystalline ice film. However, for $\theta > 30°$, the amount of N_2 adsorbed by the ASW increased markedly, reaching a maximum near $\theta = 70°$. At the maximum, the ASW films adsorbed more than 20 times the amount of N_2 adsorbed by a crystalline ice film. The quantity of N_2 adsorbed by the ASW was much greater than would be expected from a simple roughening of the surface and indicates the formation of a porous film. We have also investigated ASW films grown by filling the experimental chamber with water vapor (background dosing). In that case, the flux of water molecules striking the surface has a cosine angular distribution. The large N_2 adsorption for ASW grown by background dosing (Fig. 1) is indicative of a highly porous film and is most comparable to that obtained for ASW grown at oblique angles. Results similar to those shown in Fig. 1 were obtained for O_2 and Ar adsorbed on ASW films, indicating that the ability to adsorb large quantities of gas depends primarily on the morphology of the ASW. It is well known that the porosity of ASW and its ability to trap volatile gases depends on the growth and annealing temperatures (*7, 19–21*). However, the data in Fig. 1 show that the porosity and morphology of ASW are also strongly dependent on the angular distribution of the incident water molecules.

We estimate the ratio of N_2 molecules adsorbed to water molecules deposited in the ASW films at $\theta = 70°$ (or by background dosing) to be 1:2. This ratio is consistent with volume filling of pores by capillary condensation (*18*) and yields a density of ~0.6 g/cm^3 for the ASW film, in good agreement with earlier results (*17*). In addition, the N_2 TPD line shapes show evidence of capillary condensation (*22*).

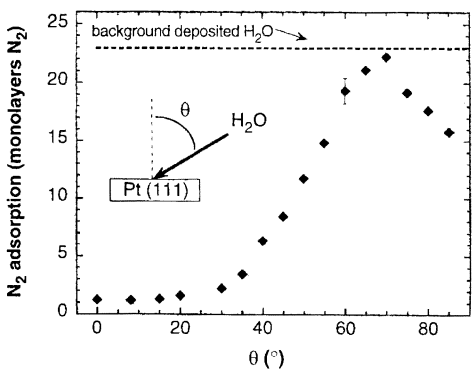

Fig. 1. Amount of N_2 adsorbed by ASW films versus θ, the angle between the incident H_2O beam and the Pt(111) surface normal. The films, which were nominally 50 bilayers thick, were deposited at 22 K. The "film thickness" corresponds to the number of bilayers that each film would have if it were grown as a nonporous crystal. The actual height of the film depends on the number of bilayers and the density, which varies with the deposition angle. The data points represent ASW films grown using a collimated, effusive H_2O molecular beam. The dashed line shows the amount of N_2 adsorbed by a 50-bilayer ASW film grown at 22 K from a random background flux formed by controlling the H_2O partial pressure in the vacuum chamber. The error bar for the data at 60° indicates the standard deviation obtained from five measurements. The error for 0° is smaller than the symbol.

Environmental Molecular Sciences Laboratory, Pacific Northwest National Laboratory, Post Office Box 999, Mail Stop K8-88, Richland, WA 99352, USA.

*These authors contributed equally to this report.
†To whom correspondence should be addressed. E-mail: bruce.kay@pnl.gov

ASW films grown at higher temperatures (*17*) or at normal incidence (*16*) have densities as high as 0.93 g/cm^3. The decrease in N_2 adsorption for $\theta > 70°$ may result from the formation of larger pores that can no longer be filled by capillary condensation at 26 K. Alternatively, the ASW structures grown at very oblique angles may be structurally weak, leading to some collapse of the films.

Figure 2 shows the N_2 adsorption by ASW grown at 22 K versus film thickness for various deposition angles. For off-normal deposition angles, the N_2 adsorption increases approximately linearly with film thickness. The adsorption of N_2 by the ASW films grown by background dosing is greater than that of the corresponding ASW films grown with collimated beams. The linear increase in N_2 adsorption, in conjunction with the magnitude of the adsorption, suggests that the pore structure in the ASW films is highly connected, allowing the N_2 to diffuse throughout the ASW film. In contrast, the amount of N_2 adsorption on ASW films grown at normal incidence is nearly independent of film thickness and similar to the amount of N_2 adsorption on the clean Pt(111) substrate, indicating denser films without a connected network of pores. In this case, N_2 adsorption occurs primarily on the external surface of the film.

We also measured N_2 adsorption by 50-bilayer ASW films as a function of the sample temperature during H_2O deposition (Fig. 3). In all cases, N_2 adsorption by the ASW films decreases with increasing surface temperature. For ASW films grown at or near normal incidence, the decrease in N_2 adsorption versus temperature is small; these films are nonporous independent of growth temperature. However, for ASW films grown at oblique angles or by background dosing, the porosity and the N_2 adsorption are strongly dependent on temperature. Above ~90 K, all ASW films, independent of the angular distribution of the incident water molecules, have essentially the same N_2 adsorption as the crystalline reference state at 145 K. We have also found that the porosity of ASW films grown at 22 K depends on the annealing temperature and time, in agreement with earlier reports that annealing reduces the porosity of ASW (*7, 8, 20*).

The data in Fig. 3 show that the morphology of vapor-deposited ASW is a complicated function of both the temperature and the angular distribution of the incident water molecules. In addition to these variables, the morphology of ASW may also depend on whether the water beam is supersonic or effusive. Using supersonic expansions, which leads to water cluster formation in the beam, apparently produces porous ASW even at normal angles of incidence (*23, 24*).

Typically, BET isotherm measurements made with N_2 at ~77 K have been used to characterize the apparent surface area of ASW. However, because the porosity is a sensitive function of the thermal history of the ASW, BET measurements should not be used to study the very fragile low-temperature deposits. Figure 3 shows that the porosity of ASW at low temperatures can be substantially higher than at 77 K. Furthermore, because the slope of the curves in Fig. 3 is nonzero at the lowest temperature of this study, ASW films grown at temperatures below 22 K are likely to have even greater porosity. For ASW films grown by background dosing, the amount of N_2 adsorbed corresponds to an apparent surface area of ~2700 m^2/g at 22 K and ~640 m^2/g at 77 K. Mayer and Pletzer obtained a value of ~420 m^2/g at 77 K using standard BET techniques (*7*). The large apparent surface areas we observe at low temperatures and oblique angles of incidence result from both large internal surface areas and N_2 multilayer formation in the pores of the ASW film.

Our observations can be qualitatively understood using a simple physical picture based on ballistic deposition (*25*). For ballistic deposition simulations of surface growth, randomly positioned particles are brought to a surface with straight-line trajectories and the particles stop as soon as they encounter an occupied site ("hit and stick"). These models lead to the formation of porous films whose morphology is strongly dependent on the angle of deposition of the particles (*25, 26*). For off-normal deposition angles, regions that are initially thicker by random chance have higher growth rates and shadow the regions behind, leading to the formation of a porous film. The shadowing effect increases as the angle of incidence increases. The formation of porous, columnar films by oblique deposition has been demonstrated for a variety of structurally stable, high-melting-point solids such as metals, oxides, and semiconductors (*27*). The control of the morphology attainable in these materials with glancing angle deposition is nicely demonstrated in recent work by Robbie *et al.* (*28*).

In the ballistic deposition models, the density decreases as the angle of incidence increases, in qualitative agreement with our experimental observations at low temperatures. For background dosing, the shadowing effect also leads to porous films with a different pore structure. The densification observed with increasing growth or annealing temperatures (or both) is a result of increased surface and bulk diffusion of the water molecules. Quantitative understanding of this diffusive behavior requires detailed molecular-level information such as that provided by molecular dynamics simulations (*29*).

Controlling the morphology of ASW by the method of deposition has important implications for experimental studies concerning the physical and chemical properties of ASW. For example, apparently conflicting results for the density of ASW versus growth temperature as measured by optical interference techniques have been obtained by Westley *et al.* (*16*) and Brown *et al.* (*17*). Westley *et al.* suggested that the conflicting results may be due to the different deposition methods used for growing the ASW films. The results of both groups are consistent with our findings: Collimated dosing at normal incidence leads to compact, nonporous films with densities independent of the growth temperature (*16*), whereas for background dosing the ASW film density increases with increasing growth temperature (*17*).

In astrophysical environments, the morphology of ASW will depend on whether it forms from a directional or a diffuse source of water vapor. Directional deposition may occur, for example, in the rings of Saturn, where it has been proposed that water molecules sputtered from the outer rings accumulate on the inner rings (*2*). Directional depo-

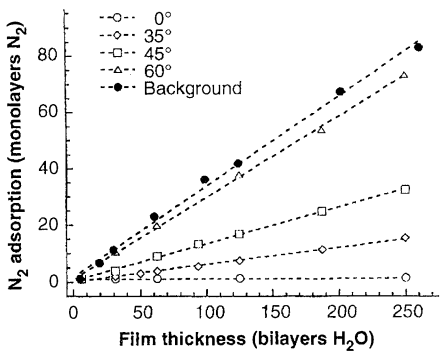

Fig. 2. Amount of N_2 adsorbed by ASW films versus film thickness. The films were deposited by collimated beams at 22 K at the angles indicated; also shown are data for ASW films grown using background H_2O dosing. Fitted lines show a linear increase in N_2 uptake with increasing film thickness.

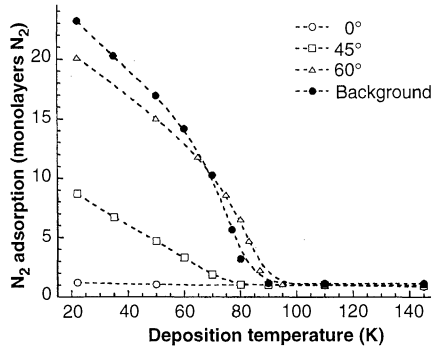

Fig. 3. Amount of N_2 adsorbed versus growth temperature for 50-bilayer ASW films. The films were deposited by collimated beams at the angles indicated; also shown are data for ASW films grown using background H_2O dosing. The dotted lines through the data are to guide the eye. For the thin films and low deposition rates used in these experiments, the ASW film temperature and the Pt(111) temperature are essentially identical ($\Delta T \ll 0.1$ K).

sition of ASW can also occur when a particle or body is passing through a water cloud with a large relative velocity. In other cases, such as the formation of comets (*1*), porous ASW may result when omnidirectional deposition of the water molecules occurs.

Adsorption, diffusion, reaction, and desorption of volatile gases on and through ASW are expected to depend critically on the morphology. These elementary kinetic processes form the microscopic basis for a variety of important astrophysical phenomena such as the outgassing of comets (*19, 20, 30, 31*) and chemical reactions in interstellar clouds (*3*). Our results show that, for porous ASW, large quantities of gases can adsorb at temperatures above the nominal equilibrium vapor pressure. The thermal conductivity of ASW, which is important in the thermal processing of icy bodies, should also depend sensitively on its morphology. The temperatures attained in the objects help to determine the extent of densification of the ASW and the diffusion, reaction, or desorption of gases trapped in the ASW. Examples of thermal processing include comets as they orbit the sun (*30, 32*) and particles in the rings of Saturn as they pass into and out of the planet's shadow (*2*).

References and Notes

1. P. Jenniskens and D. F. Blake, *Science* **265**, 753 (1994).
2. R. Smoluchowski, *ibid.* **201**, 809 (1978).
3. A. G. G. M. Tielens and L. J. Allamandola, in *Composition, Structure, and Chemistry of Interstellar Dust*, J. D. J. Hollenbach and H. A. Thronson, Eds. (Reidel, Dordrecht, Netherlands, 1986), pp. 397–469.
4. R. J. Speedy, P. G. Debenedetti, R. S. Smith, C. Huang, B. D. Kay, *J. Chem. Phys.* **105**, 240 (1996).
5. P. G. Debenedetti, *Metastable Liquids: Concepts and Principles* (Princeton Univ. Press, Princeton, NJ, 1996).
6. J. A. Ghormley, *J. Chem. Phys.* **46**, 1321 (1967).
7. E. Mayer and R. Pletzer, *Nature* **319**, 298 (1986).
8. R. Pletzer and E. Mayer, *J. Chem. Phys.* **90**, 5207 (1989).
9. A. W. Adamson, L. M. Dormant, M. Orem, *J. Colloid Interface Sci.* **25**, 206 (1967).
10. J. Ocampo and J. Klinger, *ibid.* **86**, 377 (1982).
11. M. T. Leu, L. F. Keyser, R. S. Timonen, *J. Phys. Chem. B* **101**, 6259 (1997).
12. A. H. Delsemme and A. Wenger, *Science* **167**, 44 (1970).
13. B. A. Seiber, B. E. Wood, A. M. Smith, P. R. Muller, *ibid.* **170**, 652 (1970).
14. J. A. Ghormley and C. J. Hochanadel, *ibid.* **171**, 62 (1971).
15. A. H. Narten, C. G. Venkatesh, S. A. Rice, *J. Chem. Phys.* **64**, 1106 (1976).
16. M. S. Westley, G. A. Baratta, R. A. Baragiola, *ibid.* **108**, 3321 (1998).
17. D. E. Brown *et al.*, *J. Phys. Chem.* **100**, 4988 (1996).
18. S. J. Gregg and K. S. W. Sing, *Adsorption, Surface Area, and Porosity* (Academic Press, London, ed. 2, 1982).
19. A. Bar-Nun, G. Herman, D. Laufer, *Icarus* **63**, 317 (1985).
20. A. Bar-Nun, J. Dror, E. Kochavi, D. Laufer, *Phys. Rev. B* **35**, 2427 (1987).
21. A. Bar-Nun, I. Kleinfeld, E. Kochavi, *ibid.* **38**, 7749 (1988).
22. K. P. Stevenson, G. A. Kimmel, Z. Dohnálek, R. S. Smith, B. D. Kay, data not shown.
23. E. Mayer and R. Pletzer, *J. Chem. Phys.* **80**, 2938 (1984).
24. A. Hallbrucker and E. Mayer, *J. Chem. Soc. Faraday Trans.* **86**, 3785 (1990).
25. A. L. Barabasi and H. E. Stanley, *Fractal Concepts in Surface Growth* (Cambridge Univ. Press, Cambridge, 1995).
26. P. Meakin, *Phys. Rep.* **235**, 189 (1993).
27. H. van Kranenburg and C. Lodder, *Mat. Sci. Eng.* **R11**, 295 (1994).
28. K. Robbie, J. C. Sit, M. J. Brett, *J. Vac. Sci. Technol. B* **16**, 1115 (1998).
29. Q. Zhang and V. Buch, *J. Chem. Phys.* **92**, 5004 (1990).
30. H. Patashnick, G. Rupprecht, D. W. Schuerman, *Nature* **250**, 313 (1974).
31. R. S. Smith, C. Huang, E. K. L. Wong, B. K. Kay, *Phys. Rev. Lett.* **79**, 909 (1997).
32. J. Klinger, *Science* **209**, 271 (1980).

33. Pacific Northwest National Laboratory is operated for the U.S. Department of Energy by Battelle under contract DE-AC06-76RLO 1830. Supported by the U.S. Department of Energy Office of Basic Energy Sciences, Chemical Sciences Division.

9 October 1998; accepted 27 January 1999

Semimajor Axis Mobility of Asteroidal Fragments

Paolo Farinella[1]* and David Vokrouhlický[2]

The semimajor axes of asteroids up to about 20 kilometers in diameter drift as a result of the Yarkovsky effect, a subtle nongravitational mechanism related to radiation pressure recoil on spinning objects that orbit the sun. Over the collisional lifetimes of these objects (typically, 10 to 1000 million years), orbital semimajor axes can be moved by a few hundredths of an astronomical unit for bodies between 1 and 10 kilometers in mean radius. This has implications for the delivery of multikilometer near-Earth asteroids, because the Yarkovsky drift drives many small main-belt asteroids into the resonances that transport them to the Mars-crossing state and eventually to near-Earth space. Recent work has shown that, without such a drift, the Mars-crossing population would be depleted over about 100 million years, a time scale much smaller than the age of the solar system. Moreover, the Yarkovsky semimajor axis mobility may spread in an observable way the tight semimajor axis clustering of small asteroids produced as a consequence of disruptive collisions.

Since their discovery two centuries ago, asteroids have been considered useful "test particles" for celestial mechanics. This is because asteroids are small enough ($\lesssim 10^3$ km in diameter) to have negligible gravitational influences on the sun and the planets, while also large enough that gravitation is by far the most important force affecting their orbital motion. Nongravitational forces, arising from interactions with interplanetary dust particles and solar radiation, have been thought to perturb only the orbits of small objects (*1, 2*), with diameters less than ~10 m. Two additional forces—tidal forces in planet-satellite systems and recoil forces due to gas jets from comets—are not relevant for asteroids.

Because of the dominance of gravitational perturbations by the planets, asteroidal orbits undergo long-term ($\gtrsim 10^4$ years) changes in their inclinations (i) and eccentricities (e) (*3*). In most cases, their semimajor axes (a) undergo small, short-term periodic perturbations caused by the planets. The asteroids' semimajor axes have been altered only in the so-called Kirkwood gaps in the main asteroid belt, at semimajor axes corresponding to strong orbital resonances with Jupiter, and near some other secular resonances with the outer planets. Resonant planetary perturbations have caused the asteroid population to be depleted by large eccentricity jumps leading to encounters or collisions with the planets and the sun. No other dynamical mechanism is thought to have reshaped the basic structure of the distribution of asteroidal semimajor axes since the formation of the solar system. Even disruptive collisions, which may impart to fragments relative speeds of ~100 m/s, create families of asteroids whose orbits remain tightly clustered in orbital element space (*4, 5*).

However, the Yarkovsky effect—a radiation pressure recoil force that acts on anisotropically emitting spinning bodies heated by sunlight to different temperatures in different parts of their surfaces (*2, 6*)—represents an additional force that may perturb the orbits of small asteroids (sizes up to ~20 km in diameter). The original diurnal effect, discovered by the Russian engineer I. O. Yarkovsky about a century ago, is a change in orbital elements, including the semimajor axis, of a rotating asteroidal body as a result of the diurnal changes in its surface temperature distribution. Because the "afternoon" temperature tends to be higher than in the "morning" quadrant, the thermal radiation produces a nonradial recoil force on the body.

[1]Dipartimento di Astronomia, Università di Trieste, Via Tiepolo 11, I-34131 Trieste, Italy. [2]Institute of Astronomy, Charles University, V Holesovickách 2, CZ-18000 Prague 8, Czech Republic.

*To whom correspondence should be addressed.